Multi-Objective Optimal Robust Control Scheme to Mitigate Power System Oscillations

Mahsa Kashani[1*], and Zhenyu Yang[2]

Abstract: **Given power system fluctuations, Flexible AC Transmission Systems (FACTS) can enhance stability. The Static Synchronous Compensator (STATCOM), employed for parallel reactive compensation, is a second-generation FACTS device. This paper presents a novel optimal robust scheme for designing a STATCOM damping controller, formulated as a non-dominated multi-objective optimization problem via μ-synthesis and eigenvalue analysis. To handle uncertainties, a fixed-structure controller utilizing the $\mathrm{P}-\Delta-\mathrm{K}$ configuration is applied to ensure robustness and stability. Moreover, optimal performance at the nominal operating point is treated as a primary objective alongside robust performance. A comprehensive approach is proposed for tuning the controller parameters. The proposed controller's superiority is demonstrated by comparing its performance against D-K and H_∞ controllers. Simulation results validate the effectiveness of the proposed method, showing favorable stability and robustness.**

Keywords: **Robust control, μ-synthesis, Static synchronous compensator, Dynamic stability, Optimization algorithm**

I Introduction

Flexible AC transmission systems (FACTS) can mitigate transmission line limitations, such as voltage and thermal constraints, and address power quality issues like voltage sags and harmonics [1, 2]. Low-frequency oscillations (LFOs) from parameter fluctuations and uncertain loading pose a major threat to small-signal stability, and insufficient damping may cause outages [3]. Thus, designing effective FACTS controllers is vital [4]. Robust FACTS controllers are essential to handle uncertainties, ensure stability, and dampen LFOs, while also aiming for optimal system performance. Thus, optimal robust control could be suggested as a beneficial solution to satisfy system robustness [5].

Several controlers have been proposed to design an additional damper controller (ADC) for static synchronous compensator (STATCOM) with the aims of the power system stability enhancement and voltage regulation [6, 7]. In [8], PI-based controllers to improve performance of the STATCOM and static var compensator in the face of power system oscillations. A comparison between PI and fuzzy controller to design the STATCOM-ADC was reported in [9]. In [10], a nonlinear control scheme for designing STATCOM-ADC was presented to boost the dynamic and transient stability of the power grid. A multi-objective predictive control strategy was also introduced in [11] using the eigenvalue analysis for the dynamic stability improvement of a power system. Although the problem formulation was proposed as a multi-objective problem, it was eventually transformed into a single-objective problem.

In [12], a wind turbine-oriented adaptive robust control agent was proposed for STATCOM-ADC. A predictive control was presented by [13] to analyses for the stability of hybrid power system. A coordinated control strategy for a STATCOM integrated with HVDC system has been established in [14] and simulated by PSCAD/EMTDC software with fulfilling purposes of raising both the steady and transient stability performance. To develop transient stability of a multi-machine power system integrated photovoltaic (PV), wind, FACTS devices and power system stabilizers (PSSs), particle swarm optimization-based PI controller has been proposed in [15] to improve the performance of the FACTS devices and the PSSs system.

Diverse meta-heuristic algorithms in the literature have been implemented to design STATCOM-ADC to ensure the effectiveness of the ADC. A novel intelligent control strategy has been carried out in [16] using a combination of a new General Type-II fuzzy Logic with the teaching learning based optimization algorithm to optimally and adaptively tune gains of a PI controller. Kumar *et al.* [17] have also represented an inventive manner to mitigate LFOs as well as the voltage fluctuations in the multi-machine power system aggregated with STATCOM by using ant colony optimization for the optimal adjusting of the PI controller parameters. Devarapalli *et al.* [18] have suggested a multi-verse optimizer algorithm for tuning the parameters of the PSS and STATCOM-ADC to minimize the LFOs of the power system. A solar PV-wind hybrid micro-grid in presence of STATCOM device has been modeled in [19].

Designing the STATCOM-ADC for the different systems has been pay particularly attention by researchers in recent years and different objectives have been employed as cost function to present the problem of ADC designing in the optimization problem framework. In this regard, Peres *et al.* [20] have given a single-objective opti-

[1] Department of Energy Technology, Aalborg University, Denmark
[2] Department of Energy Technology, Aalborg University, Denmark
* Corresponding Author, Email: ce.kashani@gmail.com

mization problem to tune the parameters of ADC, aiming at maximizing the minimum damping ratio. Moreover, coordinated robust control strategy for both rotor angle and voltage oscillations damping has been proposed in [21, 22] by minimizing the H_∞-norm of the closed-loop transfer function.

Regarding some complex features of the power system such as nonlinearity, load uncertainty and variable operating points, achieving stable response of the voltage and frequency regulation is challenging. Hence, to guarantee the effective response of the closed-loop system, a robust control scheme is applied to cope with the system uncertainties. In [23], a multi input-multi output robust controller has been designed based on μ-synthesis method for the nonlinear model of permanent magnet synchronous motor. A novel robust controller H_∞ and μ-analysis methods with structured uncertainties as P-Δ-K representation have been carried out in [24] for ensuring the robust performance and adjusting the terminal voltage by employing the Automatic Voltage Regulator (AVR) system. The result of simulating indicates the merit of the proposed robust controller in comparison with other optimized controllers such as traditional PID, fractional-order PID, fuzzy+PID, and interval Type-2 fuzzy logic in a wide range of the system uncertainties. Faraji *et al.* [25] have investigated two robust control strategies involving H_∞ robust control and sliding mode control to switch various operation conditions for a nonlinear multivariable model of the DFIG wind turbine.

A Contributions

By reviewing the literature, it can be seen the designing problem of STATCOM-ADC has been paid attention by different control schemes and optimization problem frameworks. Nevertheless, in the literature, it has not been given a non-dominated multi-objective optimization to design STATCOM-ADC considering robustness performance and the system efficiency in the nominal operating point. This paper presents a novel robust controller based on non-dominated multi-objective optimization approach by considering μ-synthesis method and eigenvalues analysis. The proposed controller is considered as a fixed-structured controller and its coefficients are the decision variables of the proposed optimization problem. To solve the proposed optimization problem, firstly, the Pareto optimal front is found by Non-dominated Sorting Genetic Algorithm-II (NSGA-II). Then, to determine the most preferred solution with the best compromise between the objective functions, Linear Programming Technique for Multidimensional Analysis of Preference (LINMAP) method is performed. An important advantage of the proposed multi-objective design is that it can adjust the controller coefficients according to the decision maker's preferences. In summary, we introduce such a fixed-structure controller via µ-synthesis and eigenvalue analysis, handling structured parametric uncertainty and unstructured errors from reduction, linearization, and operating-point shifts. Coefficients are optimized using NSGA-II for the Pareto front and LINMAP for compromise selection, enabling preference-based tuning.

II System modeling and problem formulation

To analyze the local oscillations of the power system, Single Machin Infinite Bus (SMIB) model is widely applied. Fig. 1 reveals a SMIB system connected to STATCOM, which is installed at the middle point in a transmission line. It consists of a step-down transformer (STD) with a leakage reactance $\mathbf{X}_{\mathrm{SDT}}$, a three-phase GTO-based voltage source converter (VSC), a DC capacitor. From Fig. 1, STATCOM-ADC system generates the control signal of the compensator by considering the power deviation as input signal. Here, fifth-order model of the SMIB with STATCOM system is employed. In the follow-up, the dynamic equations have been formulated for each component of the system.

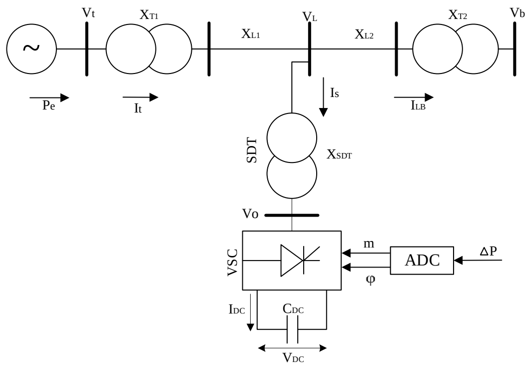

Figure 1. Schematic of a STATCOM installed in the power system.

A Synchronous generator (SG) model

In general, Park's equations, in which the axes of the machine are specified by using the d-axis and q-axis, are used to mathematically represent the SMIB system connected to STATCOM. The SG of this system is modeled by the dynamic of the q-axis transient voltage, the exciter voltage, and the electromechanical swing equations. The dynamic of the generator's internal voltage is given by:

$$\dot{e}'_q = \left[E_{fd} - e'_q - (x_d - x'_d)I_{td}\right] \frac{1}{T_{d_0}} \qquad (1)$$

where x_d, x'_d and T'_{d_0} are the d-axis synchronous reactance, transient reactance, and open circuit transient time constant, respectively. Moreover, e'_q is the voltage behind the transient reactance, and I_{td} is the SG terminal current along the d-axis. The voltage of SG exciter E_{fd} would be controlled by Automatic Voltage Regulator (AVR) system. The dynamic model of the exciter system is defined by 2, where K_A and T_A are the gain and time constant of AVR system, respectively. Moreover,

V_t is SG terminal voltage.

$$\dot{E}_{fd} = -\frac{1}{T_A}E_{fd} + \frac{K_A}{T_A}(V_{t0} - V_t) \quad (2)$$

In (2), the SG terminal voltage could be defined based on the SG terminal current as follows:

$$V_t = \sqrt{v_{td}^2 + v_{tq}^2},\ v_{td} = x_q l_{td},\ v_{tq} = e'_q - x'_d l_{tq} \quad (3)$$

The electromechanical swing equations can also be written for rotor angle δ and angular frequency ω as two first-order differential equations presented by (6) and (7).

$$\dot{\delta} = \omega_0\omega, \quad \dot{\omega} = \frac{1}{2H}[P_m - P_e - K_D\omega] \quad (4)$$

in which P_m and P_e are the mechanical and electrical power, respectively. H is the inertia constant and K_D is also machine rotor damping. SG electrical power is calculated as follows:

$$P_e = V_{td}I_{td} + V_{tq}I_{tq} \quad (5)$$

B STATCOM model

The voltage difference between V_0 and V_L causes to exchange active and reactive power between STATCOM and power system. Moreover, the AC voltage ($V_0 = mV_{DC}\angle\psi$) behind the leakage reactance of STD is controlled by the VSC system. Where, V_{DC} is DC link voltage, and m as well as ψ are control references. The dynamic of DC link voltage is formulated as follows:

$$\dot{V}_{DC} = \frac{I_{DC}}{C_{DC}} = \frac{m}{C_{DC}}\left(I_{sd}\cos\psi + I_{sq}j\sin\psi\right) \quad (6)$$

The nonlinear model of the SMIB system with STATCOM could be defined by the set of equations (1), (2), (6), (7) and (9). Considering the relationship of the currents injected by SG and STATCOM introduced by [18], the state space model of the system can be extracted in which, the state variables vector is $[\delta, \omega, e'_q, E_{fd}, V_{DC}]$ and the control variables vector is $[m, \psi]$. In order to design the proposed controller, the linearized model of the system is employed, which it has been discussed in detailed in the Appendix I.

III Robust Controller Design

One of the main aims of controller designing for the proposed system is not only stabilize the nominal system, where some elements are unmodeled or some dynamics may be neglected, but also stabilize the actual system. The controller designing by considering uncertainties is well-known as a robust control problem, in which H_∞-based control and μ-synthesis methods are mainly implemented to reach a proper robust controller. In this paper, to ensure the robust performance of the proposed controller μ-synthesis method is applied.

A System uncertainty modeling

Due to the uncertainty characteristics of the STATCOM, the system controller should be designed to ensure the system stability and performance under different operating points. To indicate the system uncertainties, an additive perturbation model is employed. The standard feedback control system with the additive perturbation is displayed in Fig. 2, in which W_s and W_u are performance and control effort weighting function. Moreover, W is a transfer function for normalizing the plant uncertainties, which it should be stable and minimum phase. The proper adjustment of weighting functions is one of the most critical aspects of robust optimization problems. The weighting function W should be designed according to the relation between the nominal system and the perturbed system. By using $\|\Delta(j\omega)\| \le 1$, it implies that:

$$\left|\frac{G_p(j\omega)}{G_0(j\omega)} - 1\right| \le |W(j\omega)| \quad (7)$$

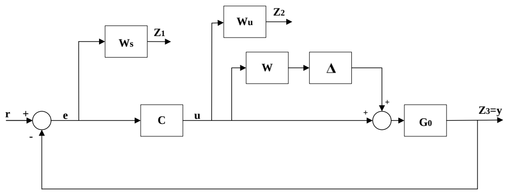

Figure 2. Feedback system with additive perturbation.

Due to the fact that neglected dynamics often occur at high frequencies, a high-pass filter could be used as an upper bound of uncertainties. (8) presents the suitable weighting function for the proposed system. Bode diagram of the weighting function and perturbed models of the system are depicted in Fig. 3.

$$W = \frac{s^2 + 199.2s + 9917}{s^2 + 200s + 10000} \quad (8)$$

The control effort weighting function is usually selected as a simple case presented by (9), in which W_u is equal to a constant value that is adjusted to prevent excessive enhancement and limit the control effort.

$$\|W_u(s)\|_\infty = \|W_u KS\|_\infty < 1 \quad (9)$$

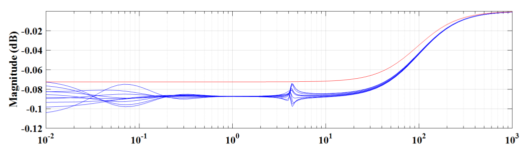

Figure 3. Bode diagram of the weighting function and perturbed models of the system.

On the other hands, the weighting function $W_s(s)$, recognized as a performance weighting function, weights a region of frequency domain to decrease the effect of disturbance on the system output. To guarantee the nominal performance $\|W_s S\|_\infty < 1$, the optimal performance weighing function can be determined as follows:

$$W_s(s) = a\frac{s^2 + 2\xi\omega_n s + \omega_n^2}{s^2 + 2\xi\omega_n s} \quad (10)$$

in which, a is regulation factor. To meet the optimal performance of the proposed system, sitting time and overshoot are assumed less than 1 second and less than 20%, respectively. Therefore, damping coefficient ζ and natural frequency ω_n are considered 0.5 and 10 rad/s, respectively. Eventually, the performance weighting function which met the requirements, is selected as follows:

$$W_s = a\frac{(s^2 + 10s + 100)}{(s + 0.05)(s + 10)(0.002s + 1)} \tag{11}$$

IV PROPOSED CONTROLLER METHOD

The proposed controller is considered as a second-order fixed-structured controller illustrated by 12. The proposed controller designing problem is defined as a multi-objective optimization approach to tune the controller coefficients, with the aim of achieving both optimal efficiency in the nominal operating point, and robust performance and stability in the worst-case conditions.

$$\frac{k_1 s^2 + k_2 s + k_3}{k_4 s^2 + k_5 s + 1} \tag{12}$$

The first objective function is defined by 13) based on eigenvalue analysis

$$f_1 = \sum_{\xi_0<\xi_i}\left[\frac{(\xi_0 - \xi_i)}{\xi_0}\right]^2 + \sum_{\sigma_0>\sigma_i}\left[\frac{(\sigma_0 - \sigma_i)}{\sigma_0}\right]^2 \tag{13}$$

in which σ_i and ξ_i are, respectively, the real part and the damping ratio for the modes which have weak-damping regarding the minimum desired mode. σ_0 and ξ_0 are the minimum of real part and damping ratio, respectively. The second and third objectives are also presented to satisfy the robust performance and stability of closed loop system based on μ-synthesis method described in last section. To minimize $\|N(s)\|_\mu$ and meet $\|N_{11}(s)\| < 1$, The second and third objective of the proposed problem are formulated as:

$$f_2 = \|N(s)\|_\mu \tag{14}$$

$$f_3 = \begin{cases} 10^5, & \text{if } \|N_{11}(s)\| \geq 1 \\ 0, & \text{if } \|N_{11}(s)\| < 1 \end{cases} \tag{15}$$

Finally, the proposed controller designing problem is given as 16 with decision variables vector $X = [k_1, k_2, k_3, k_4, k_5]$, representing the controller coefficients.

$$\begin{array}{ll} \text{Min} & F(X) = [f_1, f_2, f_3]^T \\ \text{Subject to :} & 0 \leq X \leq 500 \end{array} \tag{16}$$

V SOLUTION PROCEDURE

In this paper, to find the Pareto optimal solution set the multi-objective optimization technique has been applied. Then, multi-criteria decision-making method is employed to find best solution. Parts 1 and 2 of this section have been explained the multi-objective optimization algorithm and decision-making approach used in this paper, respectively.

A Multi-objective optimization algorithm

A non-dominated multi-objective optimization involves at least two conflicting objectives. The main aim of solving these types of problems is to obtain a set of alternate solutions, named Pareto optimal set, by simultaneously optimizing several independent objective functions. Pareto optimal set is demonstrated as 17 based on the dominance concept, for a multi-objective optimization problem.

$$\forall \text{i} \mid F_i(X_1) \leq F_i(X_2), \qquad \exists \text{j} \mid F_j(X_2) < F_j(X_1) \tag{17}$$

To reach the Pareto optimality, NSGA-II algorithm is applied in this paper. To solve the proposed problem using NSGA-II, an initial population of chromosomes is randomly determined in the problem's feasible set. Then, the fitness functions for each member are evaluated by 12–14. The selection of parents for the next generation is carried out by tournament selection method based on dominance between

B Decision-making

two members. For the two non-dominant members, the selection is done based on crowding distance. In the next step, the offspring is generated by applying crossover and mutation operators. In this paper, the two-point method is used for the crossover operator as shown in Fig. 4. After generating offspring, the elitist strategy is applied to maintain the best member from the combined populations of parents and children by considering the non-dominated sorting method.

C Decision-making

After finding the Pareto optimal set by the NSGA-II algorithm, a decision-making approach should be applied to select the most preferred solution with the best compromise between objective functions. Here, the LINMAP method has been exerted as the decision-making method of the proposed problem. This method is performed base on for main steps as follows:

Step 1: A nondimensional value $f^*_{i,j}$ is calculated for each result obtained by NSGAII algorithm as

$$f^*_{i,j} = \frac{f_{i,j}}{\sqrt{\sum_{i=1}^{N}(f_{i,j})^2}}, \quad j = 1, 2, 3 \tag{18}$$

Step 2: An unattainable ideal point based on the best results found for each objective function is determined by

$$f^*_{\text{ideal},j} = \min_i f_{i,j}, \quad j = 1, 2, 3 \tag{19}$$

Step 3: The normalized distance between each of the Pareto front results and the unattainable ideal point should be calculated by

$$d_i = \sqrt{\sum_{j=1}^{3} w_j(f^*_{i,j} - f^*_{\text{ideal},j})^2} \tag{20}$$

Step 4: The result with the lowest normalized distance is chosen as the preferred optimal solution.

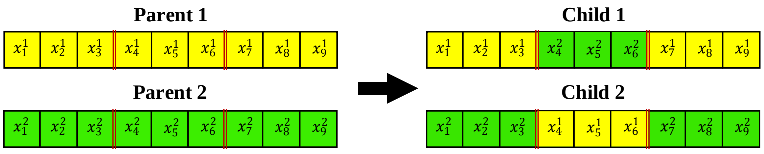

Figure 4. Demonstration of the two-point method for crossover operator.

VI Simulation and results

The proposed control scheme is introduced by multi-objective optimization problem to find optimal parameters for the proposed robust-fixed structure controller. By using the proposed controller, both robust performance and stability of the system would be insured and the controller performance in the different conditions of nominal frequency would be optimized. To evaluate the performance and stability of the proposed method, four controller are designed and the simulation results would be analyzed based on them in four cases:

- **Case 1.** μ-synthesis by using reduced D-K iteration.
- **Case 2.** Optimal H_∞ method.
- **Case 3.** The proposed method by considering priority for the robust stability and robust performance of closed-loop system. $(w_1 = 0.1, w_2 = 0.45, w_2 = 0.45)$
- **Case 4.** The proposed method by considering priority for the closed-loop system performance in nominal condition. $(w_1 = 0.8, w_2 = 0.1, w_2 = 0.1)$

Cases 1 and 2 are respectively considered to compare the robust performance and stability of the proposed controller with the controllers designed by reduced D-K iteration and optimal H_∞ method. As one of the multi-objective optimization problem advantages, the priority of each objective can be considered to achieve the most preferred solution based on the controller designer's desire by applying appropriate weighting in the decision-making method. To indicate this benefit, cases 3 and 4 are considered based on the different desires of the control scheme.

A Results and discussions

1 Controller efficiency evaluation

By considering the adjustment coefficient a = 0.005 in (17), a suitable controller based on μ-synthesis using reduced D-K iteration can be achieved for case 1. Table 1 demonstrates the results for controller designing performed by the reduced D-K iteration. As can be seen, the peak μ-value is less than 1. Therefore, the robust performance and stability condition is satisfied for this case. Figures 5 and 6, respectively, show the stability and performance of the controllers designed in different cases. For robust stability, it is required that the maximum of the μ curves at each frequency should be less than unity. As depicted in Fig. 5, all of the controllers have satisfied the robust stability for closed-loop system in the various range of frequency. It is obvious that all of the controllers have same performance robustness in low frequency as well as high frequency based on the results pictured in Fig. 6. Moreover, it can be observed, the controller designed in case 2 has better performance than others. The results obtained by case 3 and 4 have also been illustrated that structure singular value for case 3 is less than case 4 in middle frequencies. This issue shows proposed controller scheme achieves the controller goal. That means by considering a higher weighting factor for robust stability and robust performance the most preferred solution is guaranteed more robustness.

Table 1. The results for controller designing performed by the reduced D-K iteration for case 1

Iteration	2	3	4	5	6
Controller Order	13	15	17	17	17
Total D-Scale Order	4	6	8	8	8
Gamma Achieved	0.994	0.998	1.001	1.000	1.000
Peak mu-Value	0.990	0.992	0.994	0.994	0.993

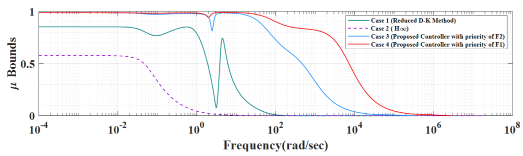

Figure 5. Structure singular value for robust stability analysis of the controllers designed in different cases.

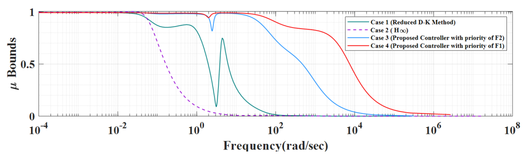

Figure 6. Structure singular value for robust performance analysis of the controllers designed in different cases.

2 Optimization efficiency evaluation

Here, NSGA-II algorithm is employed to find the pareto optimal solution. The number of members and iteration are considered 300 and 100 respectively. Fig. 7 demonstrates the Pareto front obtained by NSGA-II. Four different views of the Pareto front are displayed in this figure for better demonstration. It is noticeable that none of the Pareto solutions dominates the other and each of them are candidate as an optimal solution. In this stage, based on the designing requirements by applying a decision making method, the most preferred solution can be selected as a final optimal point.

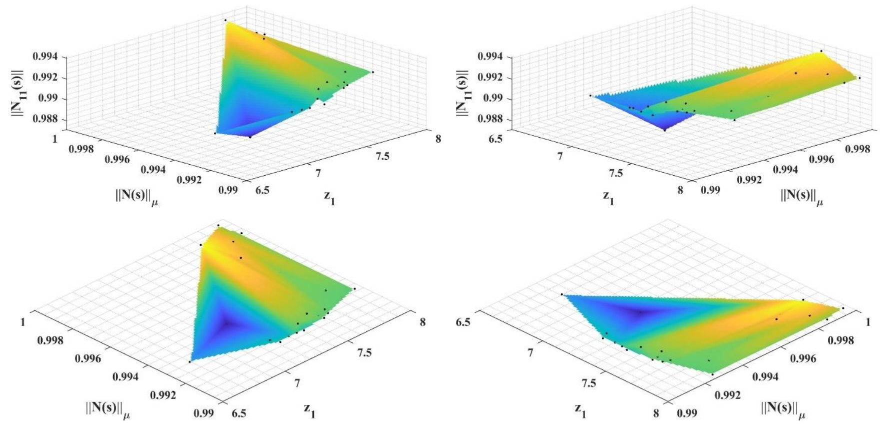

Figure 7. Pareto front of the optimal solution points from four different views.

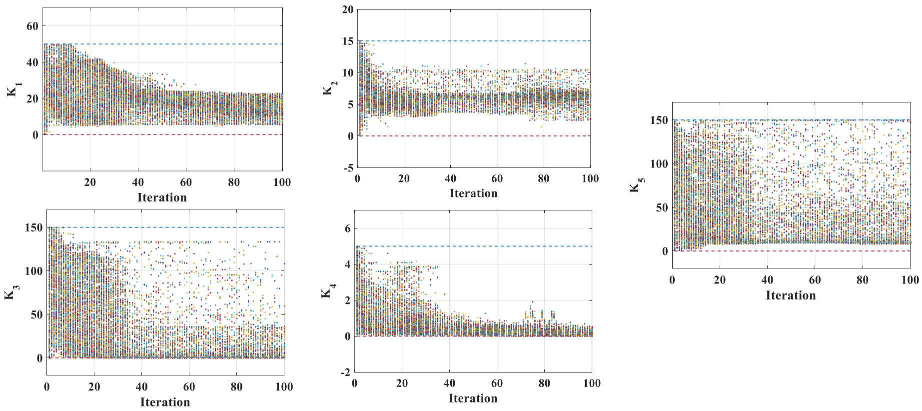

Figure 8. The scatter distribution for each parameter of the proposed controller in the different iteration.

The optimal solution chosen by LINMAP method for cases 3 and 4 is listed at Table 2. Fig. 8 indicates the scatter distribution for each parameter of the proposed controller in the different iteration of the optimization algorithm. This figure gives appropriate visual overview of the solutions, determined by each member of the population in the feasible set. It is clear that all of these solutions are within the acceptable range between maximum and minimum limit. As can be seen in this figure, in the initial iterations, the population members of the optimization algorithm search the proposed solution in the whole of the feasible set. After passing more iterations, when the heuristic optimization algorithm reaches the learning of the proposed problem, the searching of the members would be more exact. As an important outcome in the optimization, the sensitivity of the cost function to each decision variable can be observed in Fig. 8. As can be seen in this figure, almost all of the algorithm members converge to similar results for parameter k_4. This issue presents this parameter has more influence on the evaluation criteria. On the other hand, parameters k_3 and k_5 have less influence on the evaluation criteria, because the results for these parameters have been obtained in a wider range of their allowable range.

3 System evaluation

The output analysis of the closed-loop system by applying different controllers, designed by different methods, would be presented in four different states. All of the simulations are conducted on the nominal frequency of the system to investigate the controller performance in the nominal working condition. First, the nominal parameters of the system are considered. In the second case, inertia constant H is considered and other parameters are equal to their nominal values. In addition, it is supposed that damping coefficient D is 2 for the third state. In the fourth case, inertia constant H and damping coefficient D are respectively assumed 2 and 6. For all cases, a disturbance is applied as a pulse signal in second 2 of the simulation time. The rotor angle deviations for state 1 is depicted in Fig. 9. As shown in this figure, all controller can improve the system stability and controller designed by case 4 has better performance than others. This issue has been occurred due to giving priority to optimal performance in nominal conditions (i.e., first objective function). Respectively, Fig. 10 and 11 indicate the rotor angle deviations for cases 2 and 3. As it is mentioned before, in state II, the value of inertia constant H is considered two times its nominal value. By increasing the

Table 2. The results obtained by LINMAP method for the proposed system in cases 3 and 4

	Controller parameters					Objective Function		
	k_1	k_2	k_3	k_4	k_5	f_1	f_2	f_3
Case 3	6.6499	3.9746	27.3511	0.0492	48.0508	7.4103	0.9918	0
Case 4	5.7136	2.4750	34.9524	0.4928	149.7512	7.1499	0.9942	0

value of H, system stability has been decreased. Moreover, the value of damping coefficient D is considered the half of its nominal value in case 3. Here, system stability has been decreased as well. However, in both states, the proposed controller in case 4 has performed much better than other controllers. Fig. 12. shows rotor angle deviations after applying disturbance for case4. As illustrated in Fig. 13, it can be seen the system is suffering from sharp decline stability by changing H and D. The system stability reduction is so dramatic that none of the controllers are able to stabilize the system except the controller design by the proposed method in case 4 during the simulation period.

VII Conclusion

This paper proposed a fixed-structure STATCOM-ADC via non-dominated multi-objective optimization to enhance robust/optimal damping of local oscillations. Uncertainties were tackled using μ-synthesis for robust stability and eigenvalue analysis for nominal performance. NSGA-II and LINMAP yield the best trade-off. The design reduces complexity for practical use. Comparative analysis versus H_∞ and μ-synthesis with D-K iteration confirmed the proposed controller's superiority in simulations, meeting both robust stability and optimal nominal efficiency.

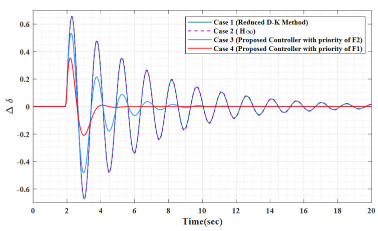

Figure 9. Rotor angle deviations after applying disturbance in state I (H=3, D=4).

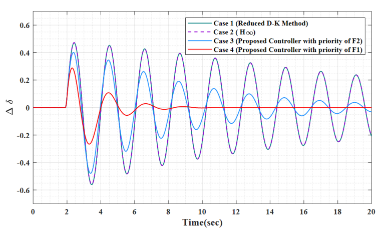

Figure 10. Rotor angle deviations after applying disturbance in state II (H=6, D = 4).

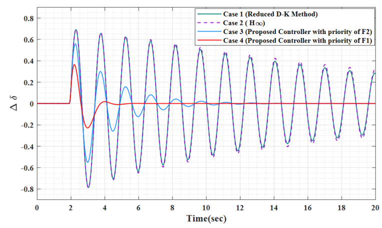

Figure 11. Rotor angle deviations after applying disturbance in state III (H=3, D = 2).

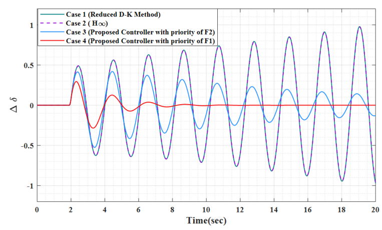

Figure 12. Rotor angle deviations after applying disturbance in state IV (H=6, D = 2).

References

[1] Gbadamosi S.L., Nwulu NI. A comparative analysis of generation and transmission expansion planning models for power loss minimization,*Sustainable Energy*, Grids Networks 2021;26:100456.

[2] Zhang, Y., *et al.* Intelligent parameter design-based impedance optimization of STATCOM to mitigate resonance in wind farms, *IEEE Journal of Emerging and Selected Topics in Power Electronics*, vol. 9, pp. 3201-15, 2021.

[3] Vetoshkin, L., Muller, Z. Dynamic stability improvement of power system by means of STATCOM with virtual inertia, *IEEE Access*, vol. 9, pp. 116105-14, 2021.

[4] Darabian, M., Bagheri, A. Design of adaptive wide-area damping controller based on delay scheduling for improving small-signal oscillations, *International Journal of Electrical Power & Energy Systems*, vol. 133, p. 107224, 2021.

[5] Alfi, A., Khosravi, M. Optimal power system stabilizer design to reduce low frequency oscillations via an improved swarm optimization algorithm, *International Journal on Technical and Physical Problems of Engineering*, vol. 4, no. 2, pp. 24-33, 2012.

[6] Leng, R. Data-driven grid-forming control for STATCOMs to achieve optimal and adaptive synchronization, *Electric Power Systems Research*, vol. 23, p. 113495, 2026.

[7] Patiño, J.E., Pareja, L.A., Carmona, O.G. Optimal placement, sizing and operation of D-STATCOMs in power distribution systems using a Mixed-Integer Linear Programming model, *Results in Engineering*, vol. 1, no. 26, p. 104749, 2025.

[8] Bhukya, J., Mahajan, V. Optimization of controllers parameters for damping local area oscillation to enhance the stability of an interconnected system with wind farm, *International Journal of Electrical Power & Energy Systems*, vol. 119, p. 105877, 2020.

[9] Faroug, M.A., *et al.* Comparative analysis of controllers for stability enhancement for wind energy system with STATCOM in the grid connected environment, *Renew Energy*, vol. 162, pp. 2408-42, 2020.

[10] Morshed, M.J., Sardoueinasab, Z., Fekih, A. A coordinated control for voltage and transient stability of multi-machine power grids relying on wind energy, *International Journal of Electrical Power & Energy Systems*, vol. 109, pp. 95-109, 2019.

[11] Darabian, M., Jalilvand, A. Improving power system stability in the presence of wind farms using STATCOM and predictive control strategy, *IET Renewable Power Generation*, vol. 12, pp. 98-111, 2018.

[12] Zhang, G., *et al.*, A data-driven approach for designing STATCOM additional damping controller for wind farms, *International Journal of Electrical Power & Energy Systems*, vol. 117, p. 105620, 2020.

[13] Darabian, M., *et al.* Stability improvement of large-scale power systems in the presence of wind farms by employing HVDC and STATCOM based on a nonlinear controller, *International Journal of Electrical Power & Energy Systems*, vol. 120, p. 106021, 2020.

[14] Wang, P., *et al.* A comprehensive improved coordinated control strategy for a STATCOM integrated HVDC system with enhanced steady/transient state behaviors, *International Journal of Electrical Power & Energy Systems*, vol. 121, p. 106091, 2020.

[15] Movahedi, A., Niasar, A.H., Gharehpetian, G.B. Designing SSSC, TCSC, and STATCOM controllers using AVURPSO, GSA, and GA for transient stability improvement of a multi-machine power system with PV and wind farms, *International Journal of Electrical Power & Energy Systems*, vol. 106, pp. 455-66, 2019.

[16] Tavana, M.R., Khooban, M.H., Niknam, T. Adaptive PI controller to voltage regulation in power systems: STATCOM as a case study, *ISA Transactions*, vol. 66, pp. 325-34, 2017.

[17] Kumar, R., Singh, R., Ashfaq, H. Stability enhancement of multi-machine power systems using Ant colony optimization-based static Synchronous Compensator, *Computers and Electrical Engineering*, vol. 83, 2020.

[18] Devarapalli, R., Bhattacharyya, B. Power and energy system oscillation damping using multi-verse optimization, *SN Applied Sciences*, vol. 3, no. 383, 2021.

[19] Bakir, H., Kulaksiz, A.A. Modelling and voltage control of the solar-wind hybrid micro-grid with optimized STATCOM using GA and BFA, *Engineering Science & Technology*, vol. 23, pp. 576-84, 2020.

[20] Peres, W., da Costa, N.N. Comparing strategies to damp electromechanical oscillations through STATCOM with multi-band controller, *ISA Transactions*, vol. 107, pp. 256-69, 2020.

[21] Kashani, M., Alfi, A. A Coordinated robust control scheme for rotor angle and voltage oscillations damping via STATCOM based on PSO, in: *28th Iran Conf Electr Eng ICEE*, pp. 9-13, 2020.

[22] Kashani, M., Alfi, A., Arabkoohsar, A. Optimal robust control scheme to enhance power system oscillations damping via STATCOM, in: *3rd International Conference on Smart Energy Systems and Technologies*, pp. 1–6, 2020.

[23] Cai, R., *et al.* Robust control of PMSM using geometric model reduction and μ-synthesis, *IEEE Transactions on Industrial Electronics*, vol. 65, pp. 498-509, 2018.

[24] Modabbernia, M., *et al.* Robust control of automatic voltage regulator (AVR) with real structured parametric uncertainties based on H_∞ and μ-analysis, *ISA Transactions*, vol. 100, pp. 46-62, 2020.

[25] Faraji Nayeh, R., Moradi, H., Vossoughi, G. Multivariable robust control of a horizontal wind turbine under various operating modes and uncertainties: A comparison on sliding mode and H_∞ control, *International Journal of Electrical Power & Energy Systems*, vol. 115, p. 105474, 2020.